Spring 2016

Alignment of neurochemically defined modules in multimodal aspects of the mouse inferior colliculus.

Chris H. Dillingham
James Madison University

Alignment of neurochemically defined modules in multimodal aspects of the mouse inferior colliculus.

An Honors Program Project Presented to

the Faculty of the Undergraduate

College of Science and Mathmatics

James Madison University

---

by Christopher Hayden Dillingham

May 2016

Accepted by the faculty of the Department of Biology, James Madison University, in partial fulfillment of the requirements for the Honors Program.

FACULTY COMMITTEE:

Project Advisor: Mark L. Gabriele, Ph.D.
Professor, Biology

Reader: Kristopher E. Kubow, Ph.D.
Assistant Professor, Biology

Reader: Derek S. Strong, Ph.D.
Assistant Professor, Biology

HONORS PROGRAM APPROVAL:

Bradley R. Newcomer, Ph.D.,
Director, Honors Program

PUBLIC PRESENTATION

This work is accepted for presentation, in part or in full, at the Association for Otolaryngology 39th Annual Midwinter Meeting on February 22nd, 2016 and at the Central Virginia Chapter of the Society for Neuroscience on March 25th, 2016.

Table of Contents

ACKNOWLEDGEMENTS:

I would like to thank Dr. Gabriele first and foremost. You have been instrumental in my time here at James Madison. I cannot express in words what you have meant to me as a mentor both academically and personally. Your patience and understanding, as well as your guidance have made you a huge part of my personal and professional life. I wish you and the lab the very best moving forward. To the junior members of the Gabriele Lab, I hope that I have been a positive role model and that you might improve on aspects where I was lacking – you are all bright and wonderful people and I have the upmost confidence that you are going great places. To Joe, who guided me to this lab and provided his own forms of mentorship – I need not tell you that you are destined for big things as you are already on that path.

To my parents, and the love and support brought me to this University, I hope you know how much you mean to me and how deeply you have contributed to the person I am today. I will always remember my time here at James Madison and value the connection our family shares with a common experience here.

To the biology faculty of James Madison, thank you for providing a foundational knowledge and background. This department has provided so many opportunities for me and I cannot express my gratitude in any other way than using my degree to work towards a brighter future in the spirit of this school. To my readers, Dr. Kubow and Dr. Strong, your feedback and patience during this process was greatly appreciated.

And finally, a caffeinated thank you to Starbucks and my roommate's Keurig machine – I could not have done this without you.

LIST OF FIGURES:

DISCLAIMER:

The present project is written in accordance with the manuscript submission guidelines for the Journal of Comparative Neuroanatomy. Additional information can be found here:

http://onlinelibrary.wiley.com/journal/10.1002/(ISSN)1096-9861/homepage/ForAuthors.html

Alignment of Neurochemically Defined Modules in Multimodal Aspects of the Mouse Inferior Colliculus.

Christopher Hayden Dillingham, Mark Lawrence Gabriele

Department of Biology, MSC 7801, James Madison University, Harrisonburg, Virginia 22807

Correspondence to:

Dr. Mark Gabriele

James Madison University

Department of Biology, MSC 7801

951 Carrier Drive

Harrisonburg, VA, 22807

gabrieml@jmu.edu

Keywords: LCIC, developmental, GAD, NADPH-d, CO, AChE

ABSTRACT:

Processing of sound requires precise coordination of various levels of the auditory system. Auditory reflexes and orientation behaviors require interactions with other systems and modalities, emphasizing the importance of highly organized integrative circuits. The inferior colliculus (IC) is a unique midbrain structure in that it exhibits aspects that are specifically arranged for processing auditory cues, as well as regions that handle multisensory inputs and thereby exhibit an entirely different organization. While the central nucleus of the IC (CNIC) is primarily auditory and arranged tonotopically, the lateral cortex (LCIC) is multimodal and exhibits a unique array of modular and extramodular fields. The present study demonstrates the postnatal presence of LCIC modular zones through immunocytochemical and histochemical approaches that stain for the neurochemical markers glutamic acid decarboxylase (GAD), acetycholinesterase (AChE), cytochrome oxidase (CO), and nicotinamide adenine dinucleotide phosphate-diphorase (NADPH-d). Results are congruent with previous findings in adult models of rat and mouse (Chernock et al., 2004; Lesicko and Llano, 2015) and reveal a distinct pattern of discontinuous modules that span midrostrocaudal LCIC Layer 2. LCIC modules are present at birth (postnatal day 0), and remain distinct through the latest stage studied, P20. Distinct modular entities are most obvious in the coronal plane at midrostrocauldal levels of the LCIC, as adjacent modules exhibit cross-bridges caudally and merge in rostral extremes of the LCIC. Alignment of various stains in serial reconstruction experiments suggest each of these markers highlight the same LCIC modular set. Morphological similarities of neurochemcial modular staining with converging projection patterns from both auditory and somatosensory centers as well as guidance expression patterns of Eph/eprhin guidance molecules in nascent LCIC indicate a functional and

developmental significance of this architecture. The present study is the first to provide several markers of the developing LCIC modular field architecture. Proper understanding of LCIC modularity may serve a role in development of therapeutic treatments of somatic tinnitus that seemingly involve multimodal LCIC circuits.

INTRODUCTION

Auditory processing is a complex physiological process involving communication between multiple levels of the peripheral and central nervous systems. It has been well documented that the auditory system demonstrates in its ascending connections a preservation of tonotopy. A tonotopic organization is a pattern in which the spatial arrangement of neurons and their innervation is based on a continuous spectrum of best frequencies corresponding to the response properties initially established in the cochlea. As signals ascend auditory centers comprising the central system, ordered frequency maps predominate and are highly conserved. One such center that in part exhibits such frequency-specific connections is the inferior colliculus (IC).

The IC is an auditory midbrain structure defined as primarily auditory that is functionally subdivided into a well-studied central nucleus (CNIC) and surrounding nuclei of the dorsal and lateral cortices (DCIC and LCIC respectively, Loftus, et. al, 2004, Loftus et al., 2008). A rich array of auditory inputs terminate within the CNIC in tonotopically organized laminar input arrangements (Merzenich and Reid, 1974; Roth et al., 1978; Semple and Aitkin, 1979; Schreiner and Langner, 1988; Kandler et al., 2009). While the largely auditory CNIC exhibits clear tonotopic frequency mapping, the neighboring LCIC and its distinct set of multimodal connections has an inherently different organization. The LCIC is further divided into three

Layers, with the most superficial Layer 1 being fibrous in nature, with cellular Layers 2 and 3. Layer 3 exhibits similarities to the CNIC, while the specific architecture of Layer 2 is less clear. LCIC inputs ascending from cochlear nucleus, descending from auditory cortex, and originating locally from the adjacent CNIC are all auditory in nature, yet lack the strict tonotopic arrangement exhibited by the CNIC. (Aitkin et al., 1981; Ryugo et al., 1981; Saldaña and Merchán, 1992; Malmierca et al., 1995; Saldaña et al., 1996; Zhou and Shore, 2006). In addition to these auditory inputs, the LCIC has been shown in a variety of adult animals to receive afferents from somatosensory structures including the spinal trigeminal nucleus (Sp5) as well as the dorsal column nuclei: cuneate and gracilis (RoBards et al., 1976; Robards, 1979; Coleman and Clerici, 1987; Wiberg et al., 1987; Weinberg and Rustioni, 1989; Shore and Zhou, 2006; Zhou and Shore, 2006). Inputs from the somatosensory centers appear to terminate in LCIC Layer 2 modular fields, while the majority of auditory inputs appear segregated, preferentially targeting surrounding portions of the LCIC classified as extramodular domains. One exception to this complementary modality framework involves auditory inputs arising from the cochlear nuclei that seemingly converge with somatosensory inputs in discrete ventral LCIC modular domains (Figure 1, Zhou and Shore, 2006). The IC is relatively preserved throughout the species discussed, sharing the three subdivisions and LCIC Layers with mouse.

Insights concerning a modular and extramodular LCIC organization stem from previous work in our lab examining Eph/ephrin expression patterns. The Eph/ephrins are a family of guidance molecules that, among other functions, help guide neuronal development and patterning of connections. Through both forward and reverse signaling mechanisms, these membrane-bound proteins instruct fine-scale decisions involving the formation of connections

between neurons. (Flanagan and Vanderhaeghen, 1998; Wilkinson 2001; Cowan and Henkemeyer, 2002; Kullander and Klein, 2002). Eph/ephrins have been shown to be instrumental in guiding auditory development, allowing for fully functioning connections to be made prior to hearing onset. In the CNIC, as well as Layer 3 of the LCIC, ephrin-B2 and EphA4 exhibit a continuous expression that guides the establishment of its frequency-based layered inputs. LCIC Layer 2 expression patterns are not graded, but rather exhibit a patchy appearance. Ephrin-B3 expression is absent in the CNIC and exhibits a complementary extramodualar LCIC pattern to ephrin-b2 and Eph-A4 (Wallace et al. 2016). These Eph-ephrin expression patterns appear qualitatively similar to the previously described multimodal modular and extramodular projection distributions seen in various tract-tracing studies. Understanding the development and emergence of this modular/extramodular architecture will aid in better understanding LCIC neural networks and the extent of multisensory integration that occurs here.

In addition to terminal patterns and Eph/ephrin expression, a host of neurochemicals that label distinct neuronal populations provide clues regarding the anatomical substrate underlying LCIC innervation. Most data on the neurochemical organization of the LCIC originates from an adult rat model, rather than developmental paradigms. (Chernock et al., 2004). Until recently the presence of neurochemically defined modules in mouse was disputed. (Lesicko and Llano, 2015). The aim of this study is to identify several neurochemical markers in developing mouse that reliably label LCIC modular fields seen in other species. The present experiments focus on glutamic acid decarboxylase (GAD), acetycholinesterase (AChE), cytochrome oxidase (CO) and nicotinamide adenine dinucleotide phosphate-diphorase (NADPH-d). GAD is an enzyme that catalyzes the conversion of glutamate into the neurotransmitter GABA. It exists in two isoforms;

GAD67, which is present ubiquitously throughout the neuron, and GAD65, localized in axons of pre-synaptic terminals. The inhibitory nature of GABA and its modular expression likely influences LCIC physiology and that of its targets, although any definitive explanation of its precise role remains speculative. NADPH-d plays a role in neuronal synthesis of nitric oxide. AChE is physiologically relevant in its breakdown of the neurotransmitter acetylcholine and is indicative of cholinergic neurons. Cytochrome oxidase is largely a metabolic marker of neuronal activity. While these individual neurochemical markers provide some information about the nature of these modular neurons, the primary goal of this study is to examine the degree of colocalization amongst markers to better understand and define LCIC anatomical compartments. Precise overlap of neurochemical markers in serial reconstructions would indicate a singular LCIC modular set. Partial overlap may be representative of a more complex mosaic of LCIC functional compartments.

MATERIALS AND METHODS

Animals

Experiments were performed on C57BL/6J control mice (n=31, Jackson Laboratories, Bar Harbor, ME). Developmental ages examined included time points prior to the onset of hearing, postnatal day 0, 4, 8, at hearing onset, postnatal day 12 (P12) and a late developmental age at P20. All procedures were performed in compliance with the National Institutes of Health *Guide for the Care and Use of Laboratory Animals* (NIH Publications No. 80-23, revised 1996) having received prior approval from the Institutional Animal Care and Use Committee. (Prot. No. A14-15)

Tissue Fixation and Sectioning

Following an overdose of ketamine (200mg/kg) and xylazine (20mg/kg), postnatal mice were transcardially perfused (physiological rinse, followed sequentially by 4% paraformaldehyde, pH 7.4 and 10% sucrose in 4% paraformaldehyde, pH 7.4). Deskulled brains were post-fixed at 4°C (4% paraformaldehyde with 10% sucrose) before transfer to a final cryoprotective solution of 30% sucrose in 4% paraformaldehyde. Fixed tissue was blocked in the coronal plane rostral to the superior colliculus (SC) and at the caudal extreme of the brainstem. Coronal sections were collected at 50μm using a sliding freezing microtome such that the entire IC was collected.

GAD Immunohistochemistry

Tissue section processing began with a quench of endogenous peroxidase activity (3% H_2O_2 in PBS for 5 min; or 0.6% H_2O_2 in PBS for 15 min), followed by three 5 minute PBS rinses. A 30 minute protein-blocking step (2.5% Normal Horse Serum) preceded an additional set of PBS rinses. A primary antibody (1:3000) made in rabbit labeling both somatic and axonal isoforms of GAD (67 & 65 respectively) was applied and agitated overnight at 4°C. Tissue was equilibrated to room temperature and rinsed in PBS in triplicate. Sections were then incubated at room temperature in an anti-rabbit IMPRESS reagent kit made in horse (Vector Laboratories MP-7401). Following another three, 5 minute PBS rinses, an ABC-DAB reaction kit was applied at room temperature (Vector Laboratories SK-4100). In some cases, when a more sensitive reaction was desired, nickel cobalt solution was added to the ABC-DAB reaction to achieve a dark black product. Addition of only primary or only secondary antibodies followed by three rinses and DAB reactions resulted in no tissue staining. A final series of 5 minute PBS rinses was

performed prior to mounting sections on gelatin-subbed slides. Sections were briefly rehydrated in dH_2O before being passed through a series of 10 minute alcohol washes (50%, 70%, 95%, 100% in duplicate) and two 20 minute xylene clearing steps. Slides were coverslipped with DPX mounting media (Sigma-06522).

Histochemistry

Tissue sections were processed for neurochemical markers AChE (n=7), CO (n=5), and NADPH-d (n=10) using procedures adapted from Karnovsky and Roots, 1964, Wong-Riley 1979, and Scherer-Singler, 1983, respectively. In cases marked for serial reconstructions, tissue was collected in grids maintaining order. Combinations of individual reactions were performed on alternative sections due to incompatibility of staining methods. Sections were mounted, dehydrated, cleared and coverslipped as described above.

Image Capture and Processing:

Brightfield image capturing was performed using a Nikon Digital Sight Color Camera (Nikon, Melville, NY). Three-dimensional Z-stacks (Elements Software; Nikon) were flattened into two dimensional images using an extended depth of field algorithm. Magnification series (4x 0.2, 10x 0.45, 20x 0.75, 40x 0.95, and 60x 1.40) were acquired and white balanced. Low magnification photomontages were made using Adobe Photoshop (San Jose, CA).

Alignments of neurochemical modular labeling of different markers in adjacent sections were performed using a MicroBrightfield Biosciences (MBF Bioscience, Williston, Vermont) neuroplotting system. Using a serial section manager in NeuroLucida software, section and modular contours were reconstructed in three-dimensions. Alignment of adjacent sections was

performed using a four-point (minimum) match of easily identifiable fiduciary landmarks in the neighboring sections. Landmarks used include easily distinguishable vasculature and midline structures: dorsal aspect of the IC commeasure, dorsal and ventral aspects of cerebral aqueduct, and the section contour of the ventral midline.)

RESULTS:

Modularity of Markers:

For each of the neurochemical markers examined, LCIC Layer 2 modules are easily identifiable (Figure 2). In mid-rostral caudal sections of the IC, distinct patches of positive cell populations are present spanning the ventrodorsal LCIC dimension. Positive modules are situated centrally in Layer 2 of the LCIC, with distinctly negative adjacent Layers 1 and 3. Equally devoid of labeling are the areas of Layer 2 between neighboring modules (Figure 3).

Developmental Emergence:

The patchwork organization of modules is apparent at all time points examined, although increasing in number and prominence at older ages (Figure 4). Modules, while evident at birth, have fewer neurons per cluster and appear less dense. Discrete modules are more easily delineated leading up to onset of hearing, and are clearly defined compartments of positive cell populations surrounded by distinctly negative Layers 1 and 3 and Layer 2 intermodular zones at postnatal day 20. This progression of density is most apparent in NADPH-d and requires further quantification (Figure 5).

Rostral-Caudal Organization:

While distinctly patchy in nature in mid rostral-caudal coronal sections, the organization of the LCIC modules is obscured towards the rostral and caudal extremes (Figure 6). In more caudal aspects presumptive patches are not discontinuous, but rather connected or bridged, resulting in a beads-on-string appearance (Figure 7). Unlike the beaded caudal organization, the rostral LCIC exhibits distinct convergence of modules into 1 to 3 positive clusters that dominate the rostral pole (Figure 8). These clusters are seen with all markers at various age points, with increasingly rostral sections containing modules appearing progressively more consolidated. This finding is in keeping with that previously described in adult rat (Chernock et al., 2004).

Neurochemical Overlap:

Preliminary NeuroLucida reconstruction alignments using fiduciary landmarks suggest potential colocalization of markers. Modules positive for NADPH-d demonstrate strong spatial registry with CO labeling in adjacent sections (Figure 9, Figure 10). Similar cases show NADPH-d overlap with AChE modules (Figure 11). Further reconstruction cases are needed to determine if each of the examined neurochemicals label the same LCIC modular set.

DISCUSSION:

Defining LCIC compartments utilizing neurochemical markers provides insights concerning LCIC structure, its developmental, and its relationship to similar neonatal Eph/ephrin guidance expression patterns. The current study demonstrates the presence of neurochemical LCIC modularity in developing mouse as previously seen in several adult species (Chernock, et al.,

2004, Lesicko and Llano, 2015). The progression from the bridged array seen in the caudal extremes to distinct entities seen mid-rostraocaudaly and finally in the convergence of modules into clusters within the rostral pole is also congruent with these previous findings (Figure 12). Modules are not only apparent at P0, but are clear entities distinctly situated in Layer 2, with non-expression in interdigitating aspects of Layer 2 and adjacent Layers 1 and 3. To fully grasp the emergence of these modules, further embryonic data is required. Future studies may also elucidate neurochemical composition of cell populations expressing the Eph/ephrin guidance molecules during these early developmental time points.

Eph/ephrin modularity:

The modularity of Eph/ephrins in the LCIC and their role in proper formation of connections is paramount in understanding proper LCIC development and circuit formation. Integration of somatosensory afferents into modular patches of the LCIC and coincident innervation by centers of both higher and lower levels of auditory processing is likely guided in part by these guidance molecules. Differential expression of various Eph/ephrins potentially orchestrates the innervation of the IC. In addition to previously described expression patterns for EphA4 and ephrins B2 and B3, several other Ephs (A6, A7, A8, B1, B2, B3, B6) and ephrins (A2 and A5) have been shown through *in situ* hybridization to be present in the nascent IC (Wallace et al., 2013; Wallace et al., 2016, www.brain-map.org). It is likely that this family of proteins plays both attractive and repulsive roles in establishing multimodal LCIC connectivity. Interestingly, expression of these guidance molecules is not restricted to patches or LCIC modules. Similar to termination patterns of afferents from auditory cortex and CNIC, ephrin-B3 is expressed in an extramodular fashion

in LCIC (Figure 13, modified from Wallace et al., 2016). Descriptions of this extramodular organization are even less well characterized; while there are multiple neurochemical markers that are demonstrative of the modularity of the LCIC, only calretinin, a calcium binding protein, has been shown to be expressed extramodularly (Lohmann and Friauf, 1996). Despite this, the utilization of neurochemical markers to define modules in LCIC creates a *de facto* separation of modular and extramodular fields.

LCIC Functionality:

The modular/extramodular arrangement of the LCIC may provide insight into its functionality. The multimodality of the LCIC has been shown in its responses to both auditory (Aitkin et al., 1975, 1981, 1994; Aitkin and Zimmermann, 1978; Syka et al., 2000; Suta et al., 2003; Ota et al., 2004) and somatosensory (Aitkin and Zimmermann, 1978; Aitkin et al., 1981) stimuli. Fields of LCIC connectivity, with primarily auditory afferents terminating extramodularly (with exception of CN) and somatosensory inputs terminating modularly, are distinct but likely not isolated, with potential for cross-talk in such proximity. In streamlining the description of LCIC modularity through neurochemical markers, precise descriptions of input and output as extramodular or intramodular can be achieved through the application of one such marker along side tract-tracing experiments. Further, the neurochemical properties descriptive of modular architecture serve to indicate potential functions. When considering the potential colocalization of GAD positive, and thus GABAergic, modules with the patchy somatosensory inputs, it follows that this organization might serve to attenuate incoming auditory stimuli. Ablations to the LCIC have been shown to increase acoustic startle responses (ASR, Parham and Willott, 1990). A possible explanation

would be that when the LCIC is removed from the central ASR pathway, the downregulating modules are destroyed, thus increasing the ASR. Inhibition of certain sounds would be evolutionarily significant in an allowance for selectivity towards non-self noises. Inputs originating from Sp5 relay somatosensory information from intraoral structures (Romfth et al., 1979; Capara, 1987; Jacquin et al., 1989; Nazruddin et al., 1989; Takemura et al., 1991; Suemune et al., 1992). Because Sp5 afferents, are modular, and modules are likely GABAergic, the LCIC organization described could explain the suppression of self-generated noise from these intraoral structures.

Tinnitus:

If proper development of the LCIC could, as proposed, lead to an attenuation of unwanted inputs, improper development could therefore lead to auditory pathologies. Disruptions to the creation of the architecture, guided in part by Eph/eprhins, or in its maintenance would likely alter the role of the LCIC. In the ablation study performed in mouse, destruction of the LCIC altered ASR response in early trials, but the normal startle response returned after several days of recovery. Neuroplasticity may have played a role in this "recovery." While such plastic rearrangements are touted as marvels of the brain, maladaptive plasticity is also a possible outcome. Tinnitus, for example, is thought to be caused in part by such maladaptation of neural connections (Engineer et al., 2013). Tinnitus is an audiological condition in which sound is perceived in the absence of auditory stimuli. The National Institute of Health estimates around 10% of the adult population in the US has experienced a bout of tinnitus in the last year (https://www.nidcd.nih.gov/health/tinnitus). While the symptoms of this condition are largely

auditory in nature, underlying causes are not always as apparent. Many cases of tinnitus are tied to age related hearing loss, however, trauma or disease can lead to what is referred to as somatic tinnitus. In this form of tinnitus, plastic rearrangements of somatosensory centers of the brain result in pathologic gain regulation in auditory pathways (Levine, 1999; Eggermont, 2005; Saunders, 2007). It stands to reason that the LCIC, receiving both somatosensory and auditory cues, plays a role in this condition. Understanding the LCICs proper organization, development and functionality may therefore be an avenue to new therapeutic approaches to debilitating diseases such as tinnitus.

CONFLICTS OF INTEREST STATEMENT:

The authors have no conflicts of interest.

OTHER ACKNOWLEDGMENTS:

Grant sponsor: National Institutes of Health; Grant number: DC012421-01; Grant sponsor: Commonwealth Research Board; Grant number: 06-09; Grant sponsor: National Science Foundation; Grant number: DBI-0619207. A special thanks to the James Madison Light Microscopy and Imaging Facility for the use of the confocal microscopy suite.

LITERATURE CITED

Aitkin L, Tran L, Syka J. 1994. The responses of neurons in subdivisions of the inferior colliculus of cats to tonal, noise and vocal stimuli. Exp brain Res 98:53–64.

Aitkin LM, Kenyon CE, Philpcyl PT, Philpott P. 1981. The Representation of the Auditory and Somatosensory Systems in the External Nucleus of the Cat Inferior Colliculus. J Comp Neurol 40:25–40.

Aitkin LM, Webster WR, Veale JL, Crosby DC. 1975. Inferior colliculus. I. Comparison of response properties of neurons in central, pericentral, and external nuclei of adult cat. J Neurophysiol 38:1196–1207.

Aitkin LM, Zimmermann M. 1978. External Nucleus of Inferior Colliculus : Auditory and Spinal Somatosensory Merents and Their Interactions. 41.

Capra NF. 1987. Localization and central projections of primary afferent neurons that innervate the temporomandibular joint in cats. Somatosens Res 4:201–13.

Chernock ML, Larue DT, Winer JA. 2004. A periodic network of neurochemical modules in the inferior colliculus. Hear Res 188:12–20.

Coleman JR, Clerici WJ. 1987. Sources of projections to subdivisions of the inferior colliculus in the rat. J Comp Neurol 262:215–226.

Cowan CA, Henkemeyer M. 2002. Ephrins in reverse, park and drive. Trends Cell Biol 12:339–46.

Eggermont JJ. 2005. Tinnitus: neurobiological substrates. Drug Discov Today 10:1283–90.

Engineer ND, Møller AR, Kilgard MP. 2013. Directing neural plasticity to understand and treat tinnitus. Hear Res 295: 58-66.

Flanagan JG, Vanderhaeghen P. 1998. The ephrins and Eph receptors in neural development. Annu Rev Neurosci 21:309–45.

Jacquin MF, Barcia M, Rhoades RW. 1989. Structure-function relationships in rat brainstem subnucleus interpolaris: IV. Projection neurons. J Comp Neurol 282:45–62.

Kandler K, Clause A, Noh J. 2009. Tonotopic reorganization of developing auditory brainstem circuits. Nat Neurosci 12:711–7.

Karnovsky MJ, Root L. 1964. A “direct-coloring” thiocholine method for cholinesterases. J Histochem Cytochem 12:219-221.

Kullander K, Klein R. 2002. Mechanisms and functions of Eph and ephrin signalling. Nat Rev Mol Cell Biol 3:475–86.

Lesicko AMH, Llano DA. 2015. Connectional and neurochemical modularity of the mouse inferior colliculus. Assoc Res Otolaryng Mtg PS-564.

Levine RA. Somatic (craniocervical) tinnitus and the dorsal cochlear nucleus hypothesis. Am J Otolaryngol 20:351–62.

Loftus WC, Bishop DC, Saint Marie RL, Oliver DL. 2004. Organization of binaural excitatory and inhibitory inputs to the inferior colliculus from the superior olive. J Comp Neurol 472:330-344.

Loftus WC, Malmierca MS, Bishop DC, Oliver DL. 2008. The cytoarchitecture of the inferior colliculus revisisted: A common organization of the lateral cortex in rat and cat. Neurosicence 154:196-205.

Lohmann C, Friauf E. 1996. Distribution of the calcium-binding proteins parvalbumin and calretinin in the auditory brainstem of adult and developing rats. J Comp Neurol 367(1):90-109

Malmierca MS, Rees A, Le Beau FE, Bjaalie JG. 1995. Laminar organization of frequencydefined local axons within and between the inferior colliculi of the guinea pig. J Comp Neurol 357:124–44.

Merzenich MM, Reid MD. 1974. Representation of the cochlea within the inferior colliculus of the cat. Brain Res 77:397–415.Roth et al., 1978

Nazruddin, Suemune S, Shirana Y, Yamauchi K, Shigenaga Y. 1989. The cells of origin of the hypoglossal afferent nerves and central projections in the cat. Brain Res 490:219–35.

Ota Y, Oliver DL, Dolan DF. 2004. Frequency-specific effects on cochlear responses during activation of the inferior colliculus in the Guinea pig. J Neurophysiol 91:2185–93.

Parham K, Willott JF. 1990. Effects of inferior colliculus lesions on the acoustic startle response. Behav Neurosci 104(6):831-840.

RoBards MJ, Watkins DW, Masterton RB. 1976. An anatomical study of some somesthetic afferents to the intercollicular terminal zone of the midbrain of the opossum. J Comp Neurol 170:499–524.

Robards MJ. 1979. Somatic neurons in the brainstem and neocortex projecting to the external nucleus of the inferior colliculus: an anatomical study in the opossum. J Comp Neurol 184:547–65.

Romfh JH, Capra NF, Gatipon GB. 1979. Trigeminal nerve and temporomandibular joint of the cat: A horseradish peroxidase study. Exp Neurol 65:99–106.

Roth GL, Aitkin LM, Andersen RA, Merzenich MM. 1978. Some features of the spatial organization of the central nucleus of the inferior colliculus of the cat. J Comp Neurol 182:661–80.

Ryugo DK, Willard FH, Fekete DM. 1981. Differential afferent projections to the inferior colliculus from the cochlear nucleus in the albino mouse. Brain Res 210:342–349.

Saldaña E, Feliciano M, Mugnaini E. 1996. Distribution of descending projections from primary auditory neocortex to inferior colliculus mimics the topography of intracollicular projections. J Comp Neurol 371:15–40.

Saldaña E, Merchán MA. 1992. Intrinsic and commissural connections of the rat inferior colliculus. J Comp Neurol 319:417–37.

Saunders JC. 2007. The role of central nervous system plasticity in tinnitus. J Commun Disord 40:313–34.

Scherer-Singler U, Vincent SR, Kimura H, McGeer EG. 1983. Demonstration of a unique population of neurons with NADPH-diaphorase histochemistry. J Neurosci Methods 9(3):229-234.

Schreiner CE, Langner G. 1988. Periodicity coding in the inferior colliculus of the cat. II. Topographical organization. J Neurophysiol 60:1823–1840.

Semple MN, Aitkin LM. 1979. Representation of sound frequency and laterality by units in central nucleus of cat inferior colliculus. J Neurophysiol 42:1626–1639.

Shore SE, Zhou J. 2006. Somatosensory influence on the cochlear nucleus and beyond. Hear Res 216-217:90–9.

Suemune S, Nishimori T, Hosoi M, Suzuki Y, Tsuru H, Kawata T, Yamauchi K, Maeda N. 1992. Trigeminal nerve endings of lingual mucosa and musculature of the rat. Brain Res 586:162– 165.

Suta D, Kvasnák E, Popelár J, Syka J. 2003. Representation of species-specific vocalizations in the inferior colliculus of the guinea pig. J Neurophysiol 90:3794–808.

Syka J, Popelár J, Kvasnák E, Astl J. 2000. Response properties of neurons in the central nucleus and external and dorsal cortices of the inferior colliculus in guinea pig. Exp brain Res 133:254–66.

Takemura M, Sugimoto T, Shigenaga Y. 1991. Difference in central projection of primary afferents innervating facial and intraoral structures in the rat. Exp Neurol 111:324–31.

Wallace MM, Kavianpour SM, Gabriele ML. 2013. Ephrin-B2 reverse signaling is required for topography but not pattern formation of lateral superior olivary inputs to the inferior colliculus. J Comp Neurol 521:1585–97.

Wallace, MN, Harris, JA, Brubaker, DQ, Klotz, CA, Gabriele ML. 2016. Graded and discontinuous EphA-ephrinB expression patterns in the developing auditory brainstem. Hearing Research 335:64-75.

Weinberg RJ, Rustioni A. 1989. Brainstem projections to the rat cuneate nucleus. J Comp Neurol 282:142–56.

Wiberg M, Westman J, Blomqvist A. 1987. Somatosensory projection to the mesencephalon: an anatomical study in the monkey. J Comp Neurol 264:92–117.

Wilkinson DG. 2001. Multiple roles of EPH receptors and ephrins in neural development. Nat Rev Neurosci 2:155–64.

Wong-Riley M. 1979. Changes in the visual system of monocularly sutured or enucleated cats demonstrable with cytochrome oxidase histochemistry. Brain Res 171(1):11-28.

Zhou J, Shore S. 2006. Convergence of spinal trigeminal and cochlear nucleus projections in the inferior colliculus of the guinea pig. J Comp Neurol 495:100–12.

FIGURE LEGENDS

Figure 1. Summary figure of input and output patterns to modular and extramodular fields of LCIC Layer 2.

Figure 2. Low magnification photomontages at P8 (**A, B**), P12 (**C**) and P20 (**D**) showing distinct LCIC Layer 2 modular labeling for AChE, NADPH-d, GAD, and CO. Scale bars = 500μm.

Figure 3. High magnification photomicrographs of characteristic Layer 2 modules (*dashed contours)* from the right LCIC of corresponding plates in Figure 1 (**A-D**). Scale bars = 100 μm.

Figure 4. Low magnification view of LCIC Layer 2 GAD-positive modules (dashed contours) at P0 (**A**), P4 (**B**), P8 (**C**), and P20 (**D**). Scale bars = 500 μm.

Figure 5. High magnification view of NADPH-d modules (dashed contours) at P0 (**A**), P4 (**B**), P8 (**C**), and P20 (**D**). Scale bar in A = 25 μm, B-D = 40 μm.

Figure 6. Caudal-to-rostral distribution (**A-F**) of NADPH-d staining in LCIC Layer 2 in coronal plane. Scale bars = 500 μm.

Figure 7. NADPH-d (**A**) and GAD (**B**) staining in caudal extent of P20 LCIC. Arrows indicate modular clusters between which neurochemically positive bridges are observed in caudal extremes. Scale bars = 200 μm.

Figure 8. Rostral extent of P4 LCIC showing clustering of NADPH-d (**A**) and AChE (**B**) modular staining (*arrows)*. Scale bars = 100 μm.

Figure 9. Summary figure of caudal-to-rostral reconstructions of adjacent P12 coronal sections stained for NADPH-d (blue) and CO (orange).

Figure 10. Reconstruction of P20 adjacent sections stained for NADPH-d (blue) and CO (orange).

Figure 11. Reconstruction of P8 adjacent sections stained for NADPH-d (blue) and AChE (orange).

Figure 12. Summary schematic of caudal-to-rostral progression of LCIC architecture. This diagram combines data from the present study as well as Wallace et al., 2016. Modular fields defined neurochemically by AChE, CO, GAD, and NADPH-d and by guidance molecules ephrin-B2 and EphA4 are shown in pink. Extramodular zones defined by expression of eprhin-B3 (and likely other markers) is defined in the midrostrocaudal segment in blue. Subdivisions of the IC and other auditory nuclei are indicated by dashed contours.

Figure 13. Figure modified from Wallace et al., 2016. Summary of X-Gal labeling (**A-C**) and corresponding brightness profiles generated from curved contour sampling along LCIC Layer 2 (**D-F**). Distinct modules (*dashed contours)* are seen in LCIC Layer 2 at higher magnification for ephrin-B2 (**G**) and Eph A4 (**H**) while ephrin-B3 expression (*dashed contour)* is complementary with labeling most concentrated in extramodular domains (**I**). Scale bars in A-C = 200µm, G-I = 50µm.

Figures:

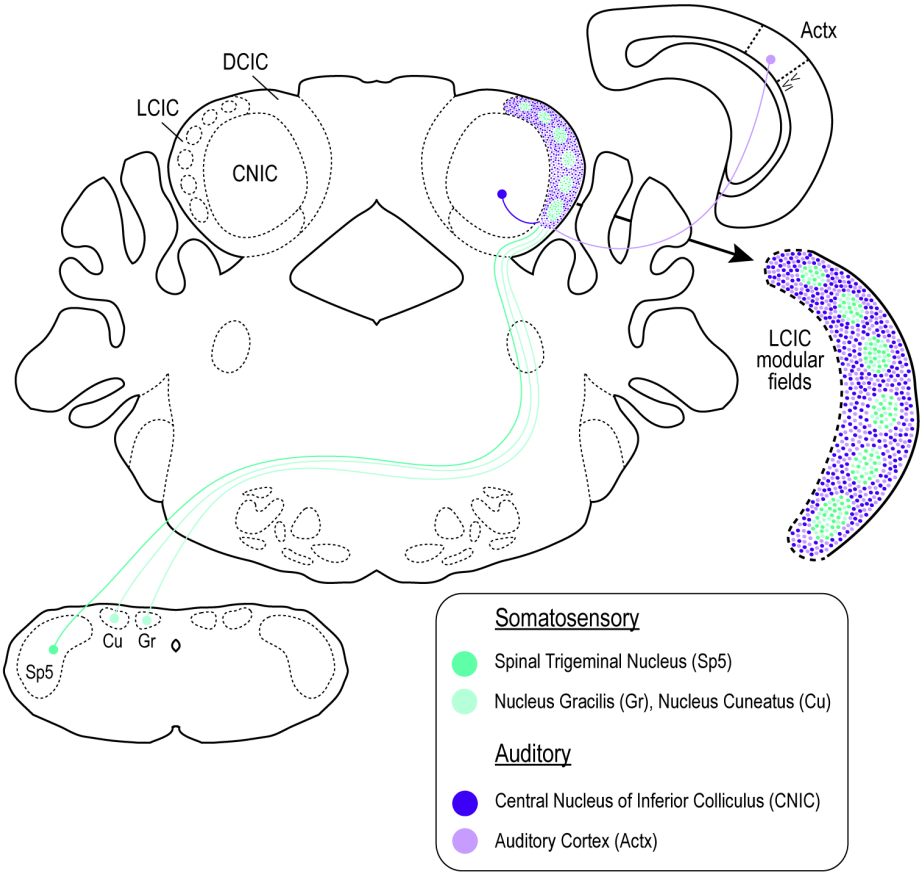

Figure 1.

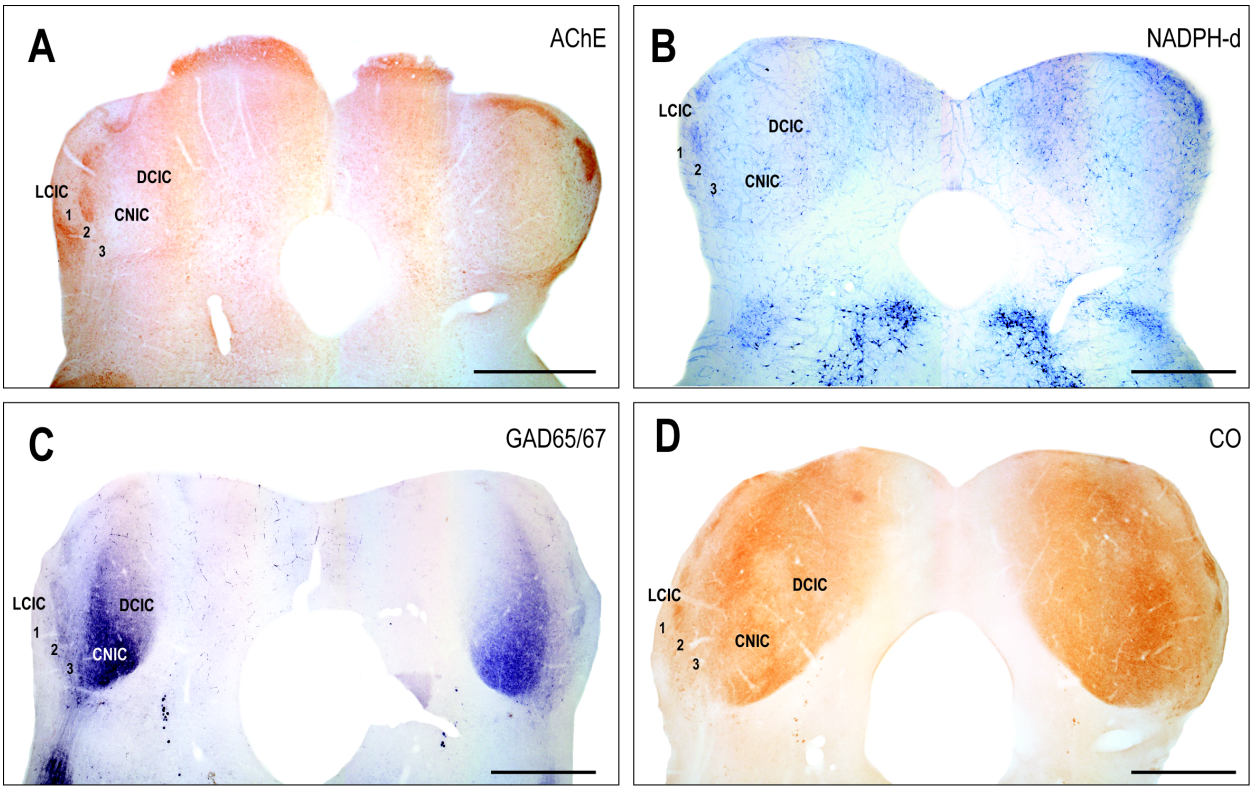
A
AChE
LCIC
DCIC
CNIC
1
2
3
B
NADPH-d
LCIC
DCIC
CNIC
1
2
3
C
GAD65/67
LCIC
DCIC
CNIC
1
2
3
D
CO
LCIC
DCIC
CNIC
1
2
3

Figure 2.

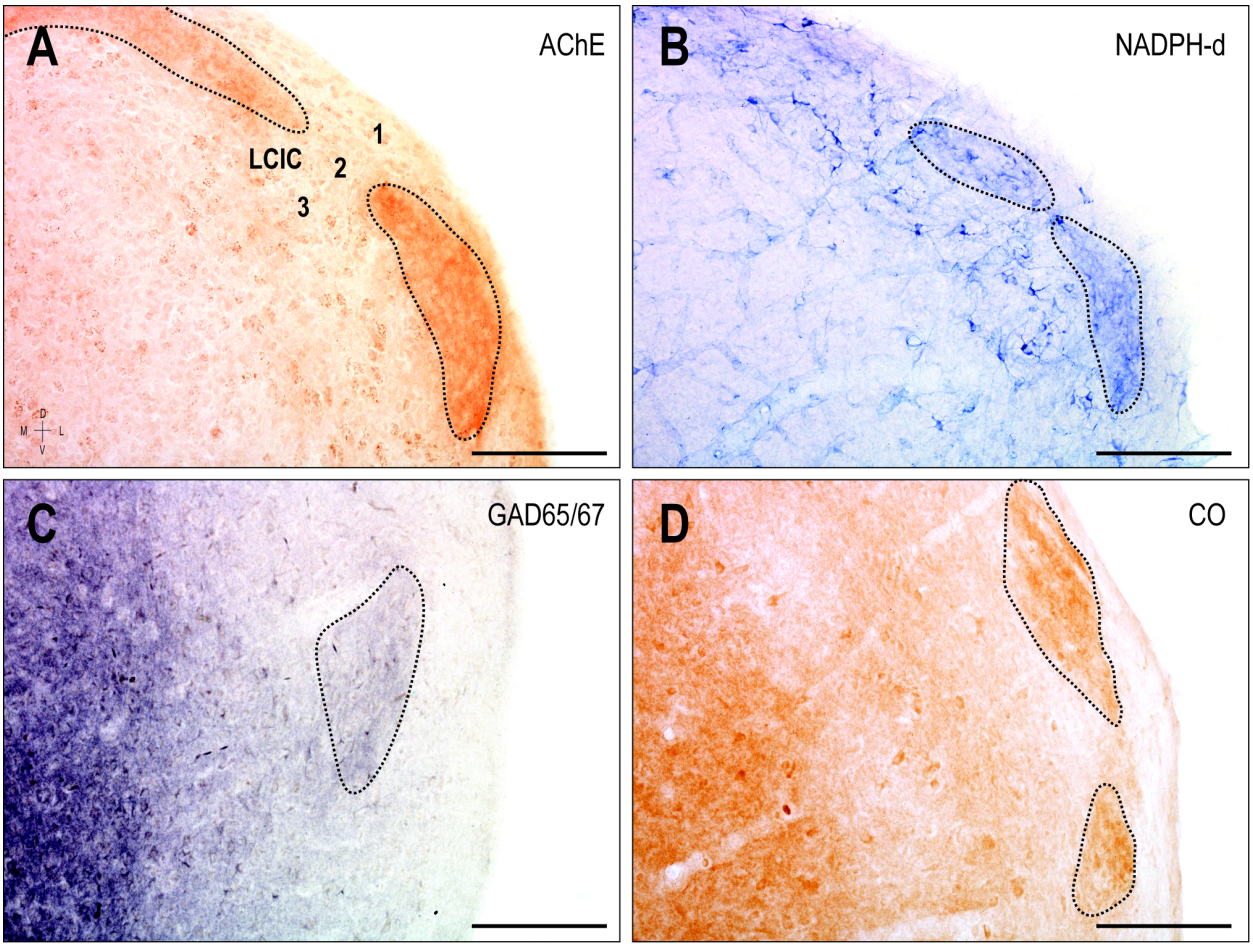

Figure 3.

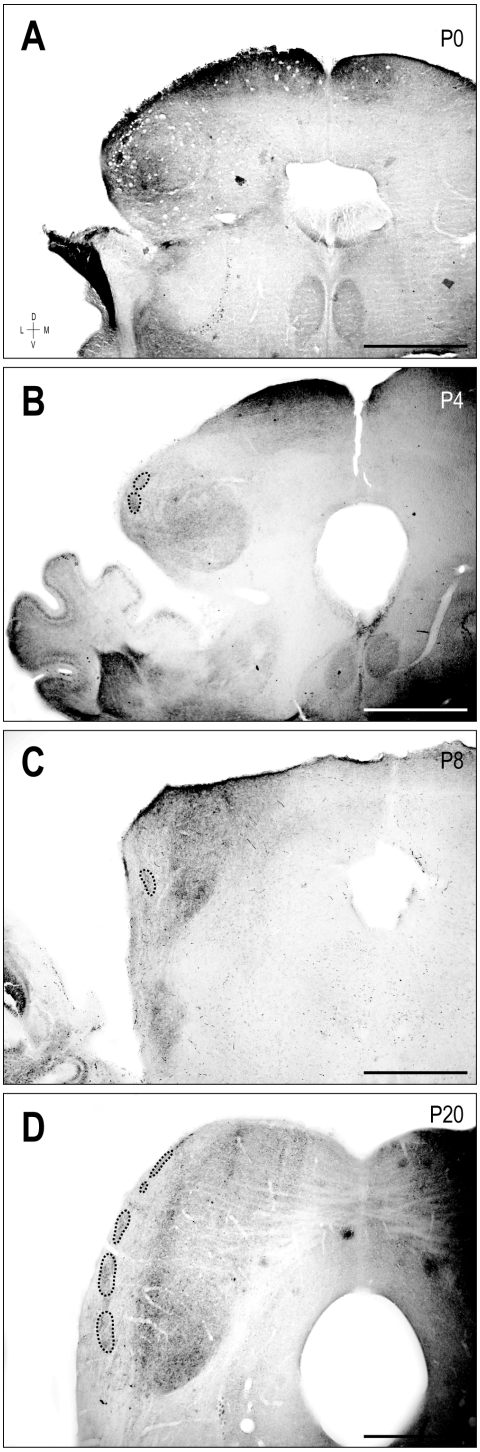

Figure 4.

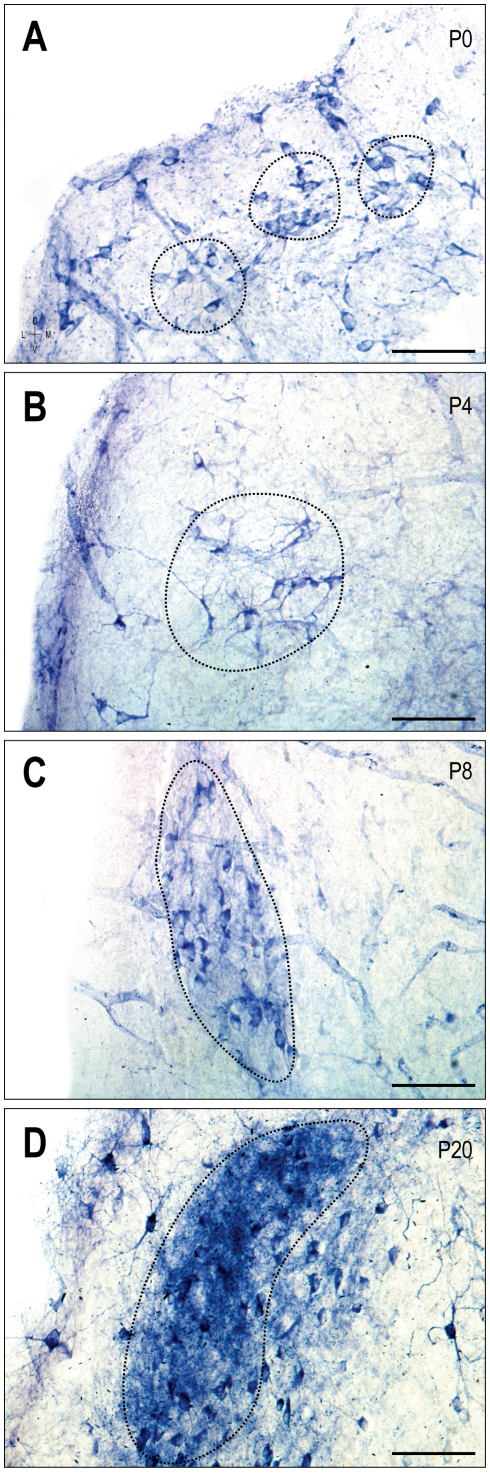

Figure 5.

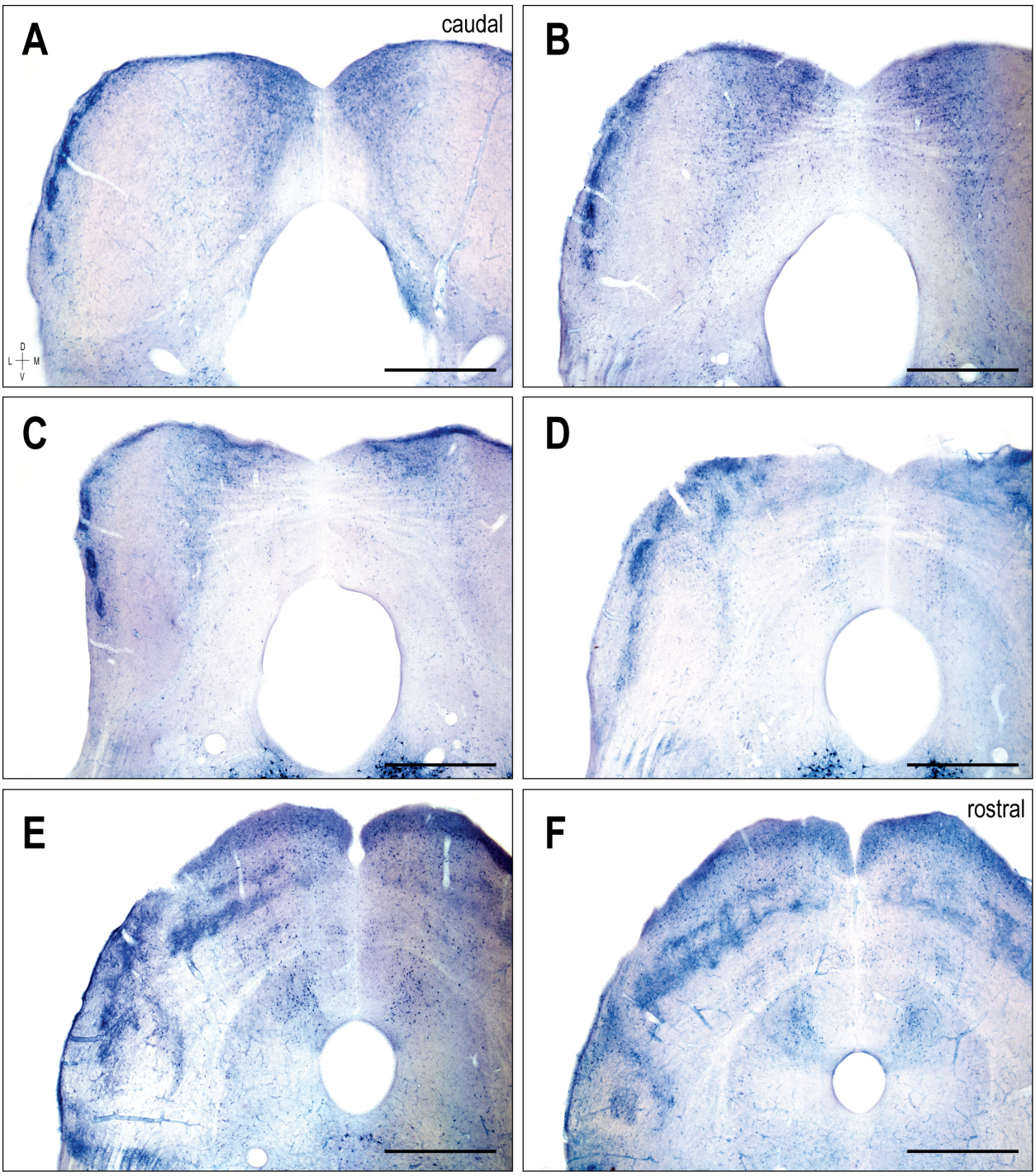

Figure 6.

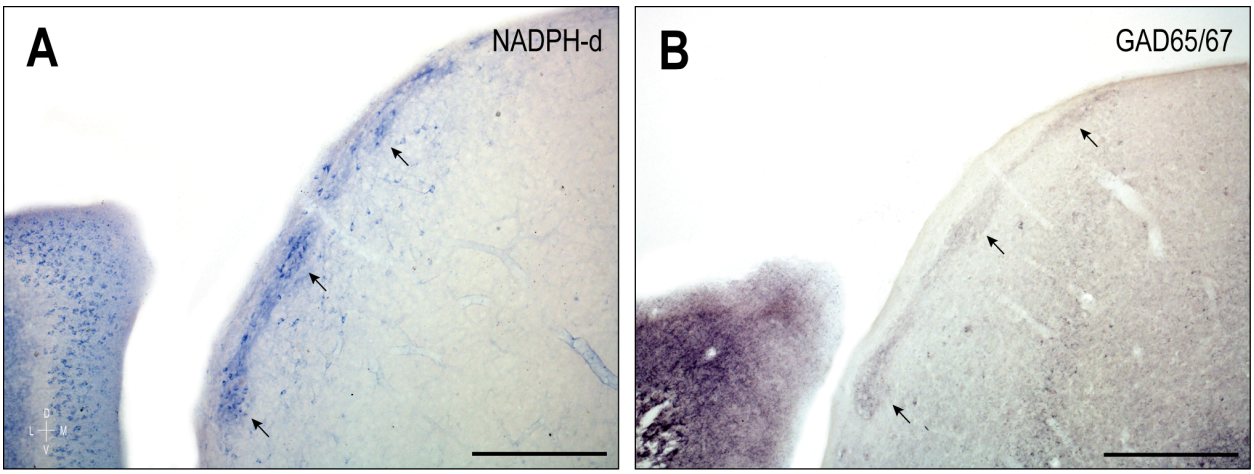

Figure 7.

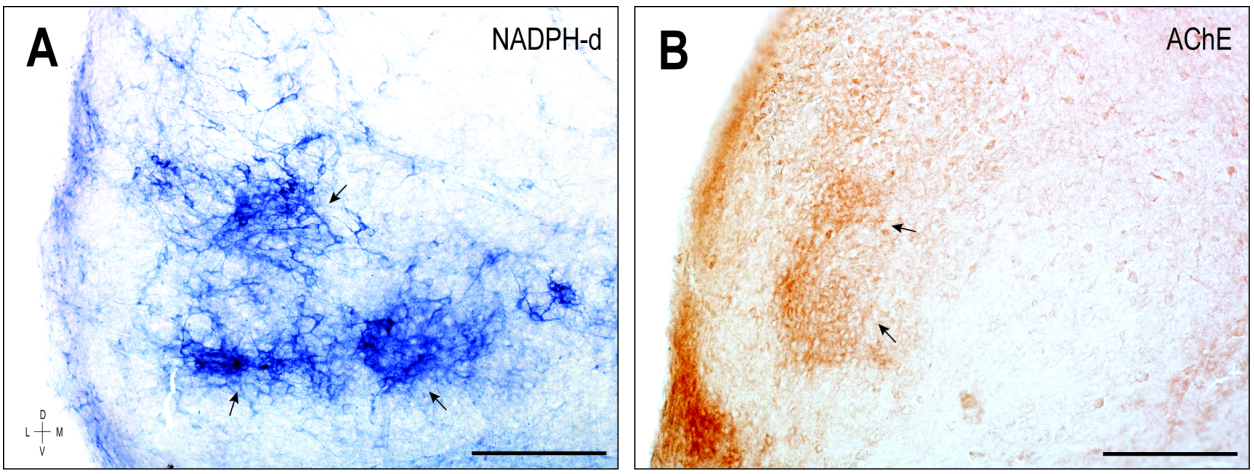

Figure 8.

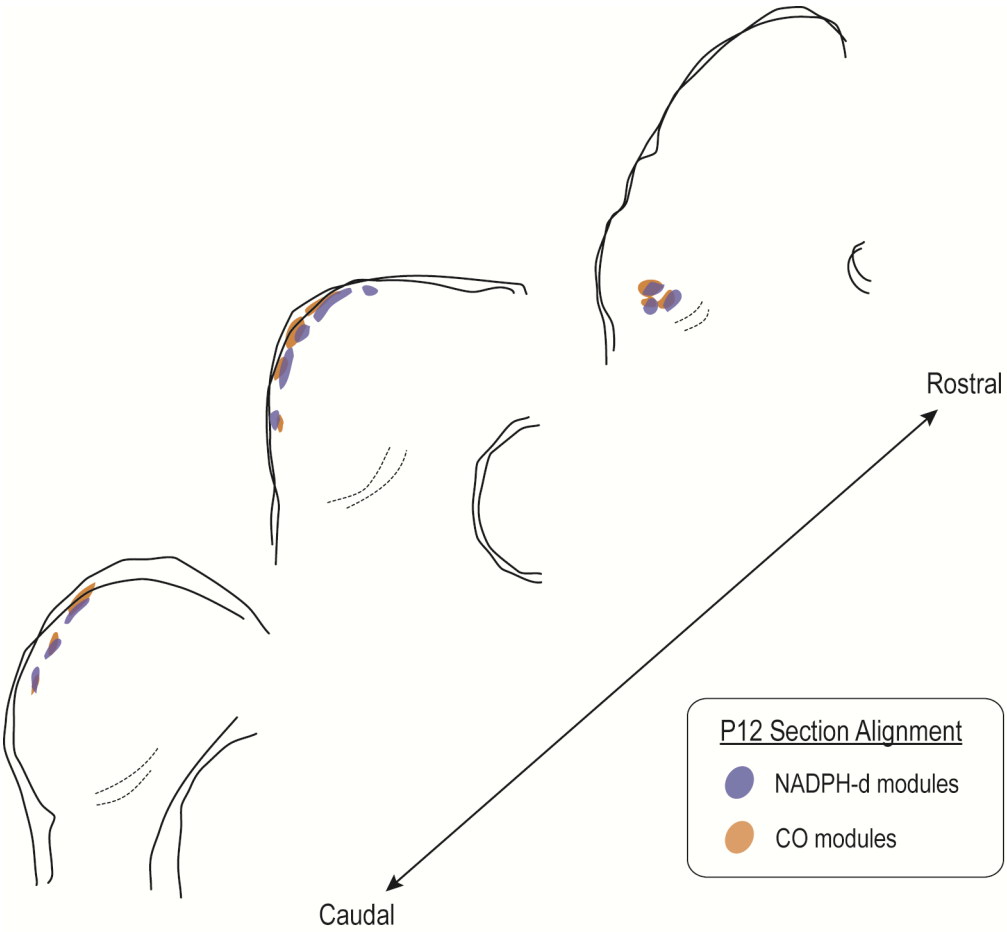
Rostral
Caudal
P12 Section Alignment
NADPH-d modules
CO modules

Figure 9.

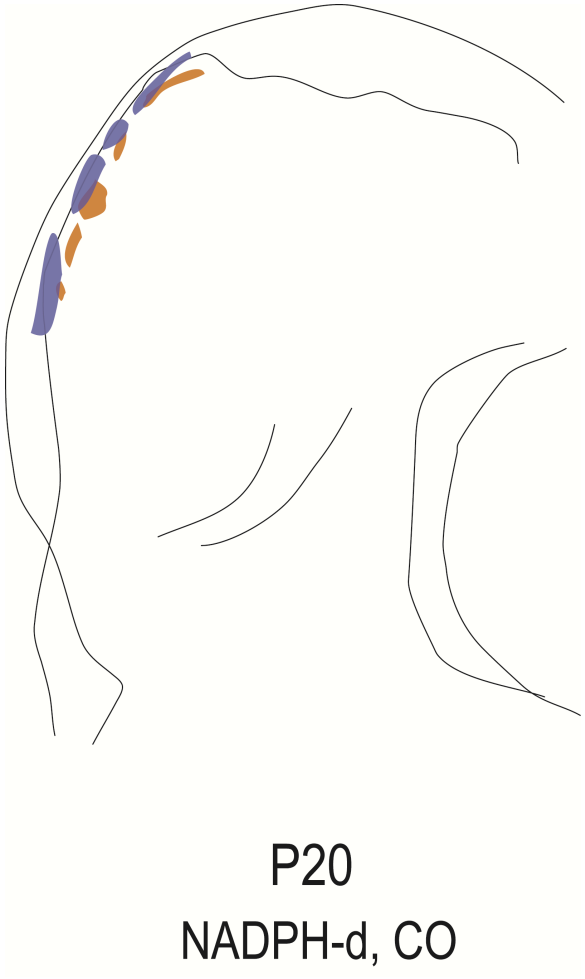

Figure 10.

Figure 11.

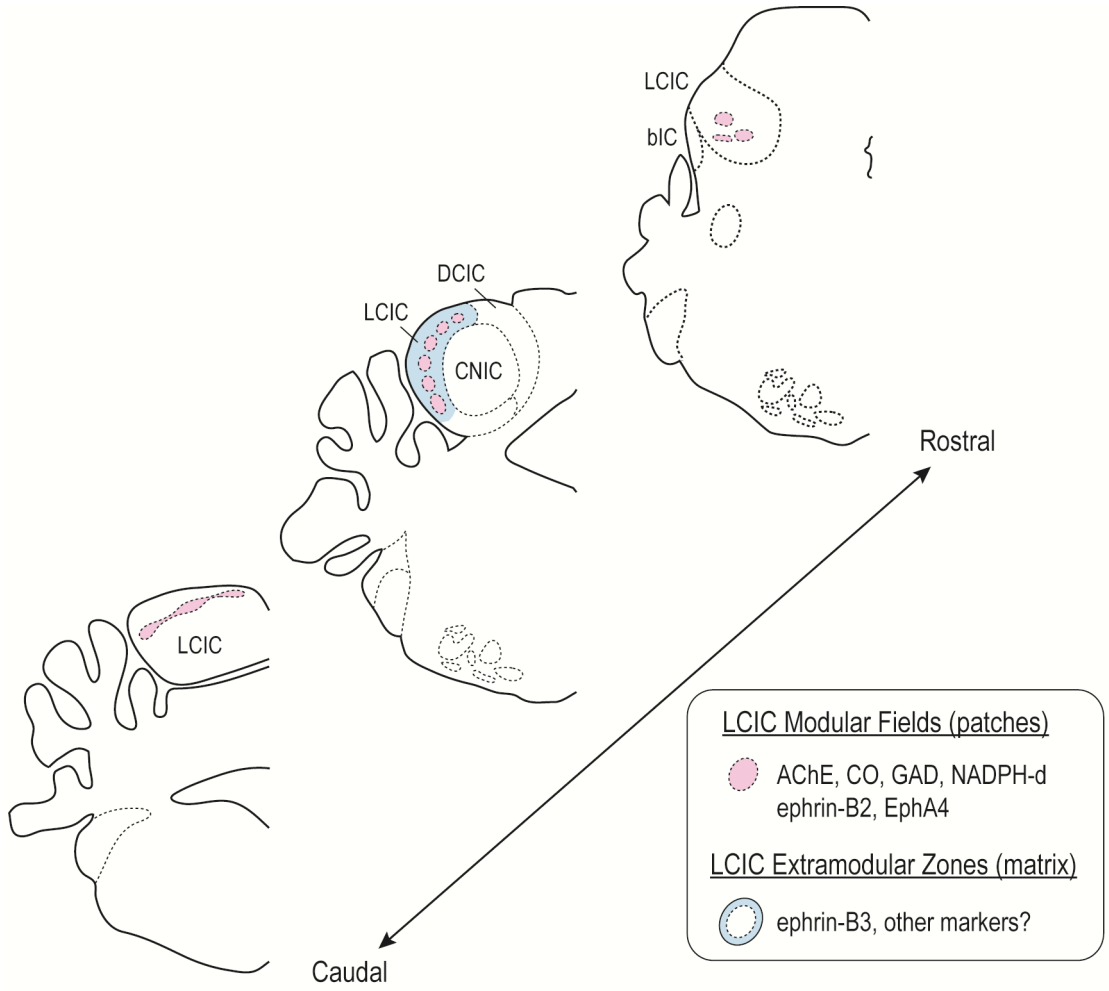
LCIC
bIC
DCIC
LCIC
CNIC
Rostral
LCIC
Caudal
LCIC Modular Fields (patches)
AChE, CO, GAD, NADPH-d
ephrin-B2, EphA4
LCIC Extramodular Zones (matrix)
ephrin-B3, other markers?

Figure 12.

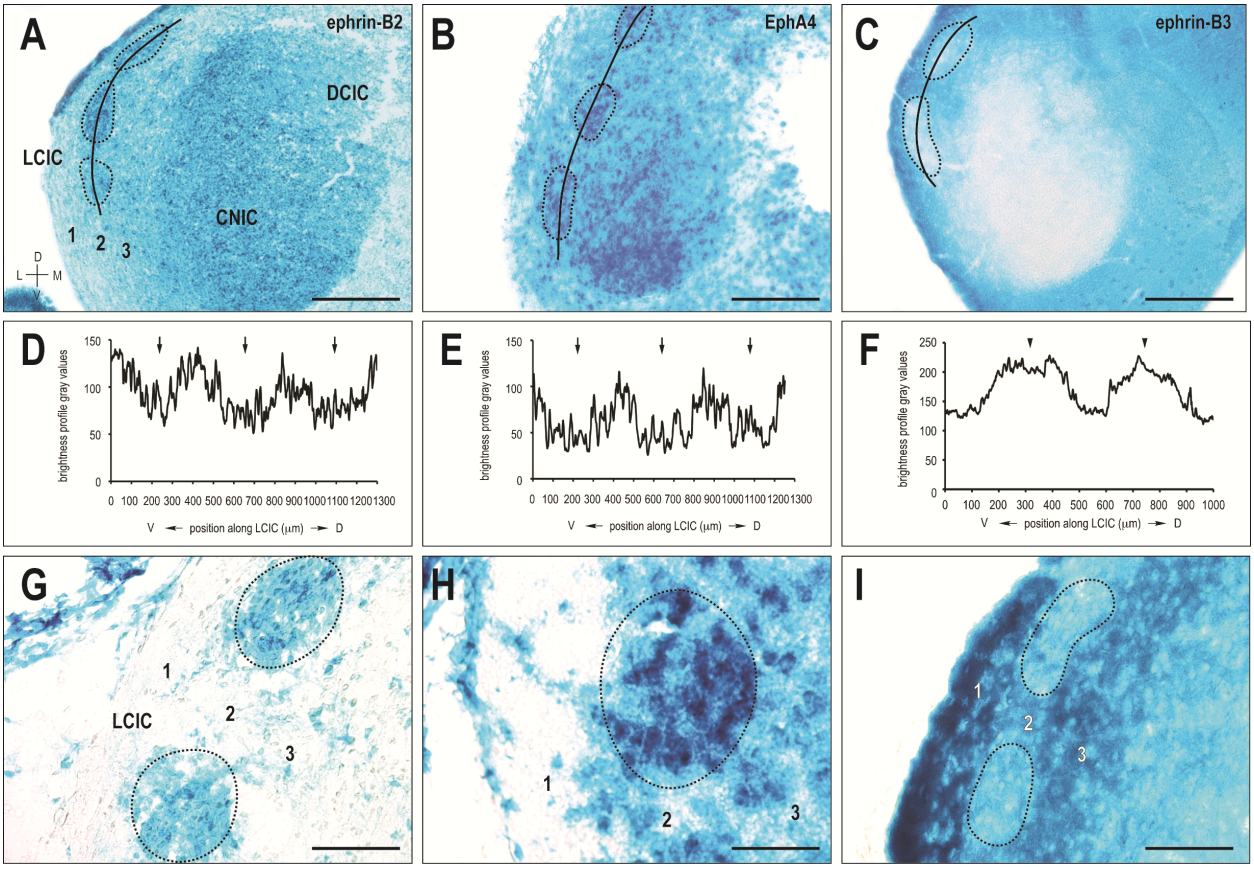
A
ephrin-B2
DCIC
LCIC
CNIC
1
2
3
D
L
M
V
B
EphA4
C
ephrin-B3
D
brightness profile gray values
150
100
50
0
0 100 200 300 400 500 600 700 800 900 1000 1100 1200 1300
V ◄ position along LCIC (μm) ► D
E
brightness profile gray values
150
100
50
0
0 100 200 300 400 500 600 700 800 900 1000 1100 1200 1300
V ◄ position along LCIC (μm) ► D
F
brightness profile gray values
250
200
150
100
50
0
0 100 200 300 400 500 600 700 800 900 1000
V ◄ position along LCIC (μm) ► D
G
1
LCIC
2
3
H
1
2
3
I
1
2
3

Figure 13.